

## CO<sub>2</sub> Conversion by Combining a Copper Electrocatalyst and Wild-type Microorganisms

ChemCatChem

Chatzipanagiotou, Konstantina Roxani; Jourdin, Ludovic; Buisman, Cees J.N.; Strik, David P.B.T.B.; Bitter, Johannes H.

<https://doi.org/10.1002/cctc.202000678>

This publication is made publicly available in the institutional repository of Wageningen University and Research, under the terms of article 25fa of the Dutch Copyright Act, also known as the Amendment Taverne. This has been done with explicit consent by the author.

Article 25fa states that the author of a short scientific work funded either wholly or partially by Dutch public funds is entitled to make that work publicly available for no consideration following a reasonable period of time after the work was first published, provided that clear reference is made to the source of the first publication of the work.

This publication is distributed under The Association of Universities in the Netherlands (VSNU) 'Article 25fa implementation' project. In this project research outputs of researchers employed by Dutch Universities that comply with the legal requirements of Article 25fa of the Dutch Copyright Act are distributed online and free of cost or other barriers in institutional repositories. Research outputs are distributed six months after their first online publication in the original published version and with proper attribution to the source of the original publication.

You are permitted to download and use the publication for personal purposes. All rights remain with the author(s) and / or copyright owner(s) of this work. Any use of the publication or parts of it other than authorised under article 25fa of the Dutch Copyright act is prohibited. Wageningen University & Research and the author(s) of this publication shall not be held responsible or liable for any damages resulting from your (re)use of this publication.

For questions regarding the public availability of this publication please contact [openscience.library@wur.nl](mailto:openscience.library@wur.nl)

# CO<sub>2</sub> Conversion by Combining a Copper Electrocatalyst and Wild-type Microorganisms

Konstantina-Roxani Chatzipanagiotou,<sup>[a, b]</sup> Ludovic Jourdin,<sup>[b, c]</sup> Cees J. N. Buisman,<sup>[b]</sup> David P. B. T. B. Strik,<sup>\*,[b]</sup> and Johannes H. Bitter<sup>\*,[a]</sup>

Carbon dioxide (CO<sub>2</sub>) can be converted to valuable products using different catalysts, including metal or biological catalysts (e.g. microorganisms). Some products formed by metal electrocatalysts can be further utilized by microorganisms, and therefore catalytic cooperation can be envisioned. To prevent cumbersome separations, it is beneficial when both catalyst work under the same conditions, or at least in the same reaction medium. Here, we will show that a formate-producing copper electrocatalyst can function in a biological medium.

Furthermore, we will show that the effluent of the copper-containing reactor can be used without purification as the sole medium for a bio-reactor, inoculated with a mixed culture of microorganisms. In that second reactor, formate, H<sub>2</sub> and CO<sub>2</sub> are consumed by the microorganisms, forming acetate and methane. Compared to simple buffer electrolyte, catalytic activity of copper was improved in the presence of microbial growth medium, likely due to EDTA (Ethylenediaminetetraacetic acid) present in the latter.

## 1. Introduction

Globally, there are ongoing efforts to recycle emitted CO<sub>2</sub> into new products like fuels, commodity chemicals, feed and food. With the envisioned future availability of a surplus of cheap renewable electricity,<sup>[1]</sup> the conversion of CO<sub>2</sub> into fuels and platform chemicals by electrocatalytic and/or bio-electrochemical conversions could be a viable approach.<sup>[2]</sup> For a sustainable electricity-driven conversion process, the actual quest is to construct catalysts that make effective use of widely available materials and can operate at high rates and with high selectivities.

Among the products of electrocatalytic CO<sub>2</sub> conversion, formate and carbon monoxide were ranked as most relevant for large-scale production as platform chemicals, based on energy requirement.<sup>[3]</sup> Both products require the transfer of two electrons, making reaction kinetics and catalyst design easier, compared to other products, such as methane or ethanol.<sup>[4]</sup>


Various studies have focused on the design of novel electrocatalysts that can achieve high selectivities for multi-electron conversions from CO<sub>2</sub> in an one-step process.<sup>[5]</sup> Alternatively, a multi-step catalytic process could be envisioned, which combines different catalysts operating in sequence (Scheme 1), to enable and/or improve the production of more complex molecules from CO<sub>2</sub>.<sup>[6]</sup> Among the types of catalysts that can reduce CO<sub>2</sub>, microorganisms are promising candidates, as they are versatile, resilient under a wide range of conditions, naturally-occurring and self-regenerating. Microbial catalysis provides opportunities on new production routes from CO<sub>2</sub>, which cannot be attained by applying a CO<sub>2</sub>-reducing electrocatalyst, such as the acetyl-CoA, glycine or serine metabolic pathways.<sup>[7]</sup> All commonly reported products during CO<sub>2</sub> electro-reduction (i.e. CO, HCOO<sup>-</sup>, CH<sub>4</sub>, C<sub>2</sub>H<sub>4</sub>, C<sub>2</sub>H<sub>5</sub>OH, H<sub>2</sub>) can be (co-)utilized in microbial metabolic processes.<sup>[8]</sup> Electrocatalytic production with metal catalysts of such intermediate products, and subsequent utilization of said products by microorganisms, would create a syntrophic relationship between the two types of catalysts. Formate in particular has the potential to become a key intermediate to link electrification and biotechnological applications due to its high solubility and low toxicity compared to CO,<sup>[4b]</sup> and it is readily convertible by a variety of microorganisms.<sup>[9]</sup>

A bio-catalytic process that leads to multi-electron transfer and longer carbon chains is microbial chain elongation. It can proceed via multiple pathways and is catalyzed by a variety of microbial functional groups.<sup>[8d]</sup> Several short carbon chains like CO<sub>2</sub> (C1), formate (C1), acetate (C2) or propionate (C3) can be elongated to medium chain fatty acids with various exogenous electron donors, such as H<sub>2</sub> and ethanol.<sup>[8d,10]</sup> Wild type, mixed (undefined) microbial catalysts are often used in these microbial chain elongation processes, which can be applied in open-culture technologies, converting real waste streams.<sup>[11]</sup> Microbial chain elongation processes were recently developed to produce caproic acid (C6); though also longer chains up to C8 and C9

[a] K.-R. Chatzipanagiotou, Prof. J. H. Bitter  
Biobased Chemistry and Technology  
Wageningen University & Research  
Bornse Weiland 9  
6708 WG, Wageningen (The Netherlands)  
E-mail: harry.bitter@wur.nl

[b] K.-R. Chatzipanagiotou, Dr. L. Jourdin, Prof. C. J. N. Buisman,  
Dr. D. P. B. T. B. Strik  
Environmental Technology  
Wageningen University & Research  
Bornse Weiland 9  
6708 WG, Wageningen (The Netherlands)  
E-mail: david.strik@wur.nl

[c] Dr. L. Jourdin  
Current address  
Department of Biotechnology  
Delft University of Technology  
van der Maasweg 9  
2629 HZ, Delft (The Netherlands)

 Supporting information for this article is available on the WWW under  
<https://doi.org/10.1002/cctc.202000678>



**Scheme 1.** Schematic of envisioned catalytic cooperation (in sequence) for the conversion of  $\text{CO}_2$ . Intermediate products, including reduced  $\text{CO}_2$  and electrocatalytically-produced hydrogen, are formed by a metal electrocatalyst, and can be further converted to longer carbon chains by a mixed culture of microorganisms (bio-catalyst).

were reported.<sup>[12]</sup> These medium chain fatty acids represent a new spectrum of platform molecules for the production of end-products such as feed additives, chemicals, dyes, solvents, plastics and fuels.<sup>[11,12b]</sup> As mentioned, some of the short chain fatty acids (e.g. formate) and electron donors used in chain elongation are shown to be produced during  $\text{CO}_2$  electro-reduction.<sup>[5f,13]</sup> By integrating  $\text{CO}_2$  electrocatalysis with microbial chain elongation, a variety of multi-carbon fatty acids can be potentially produced.

Earlier work of Li and co-workers<sup>[14]</sup> showed a first proof that catalytic cooperation of a metal electrocatalyst and bacteria was possible in a microbial growth medium. They used a pure culture of the chemolithoautotrophic bacterium *Cupriavidus necator* (formerly *Ralstonia eutropha*), genetically engineered to enable the conversion of formate to higher alcohols. Cultures of this bacterium were added in an electrochemical reactor, and were able to *in situ* convert formate, which was electrocatalytically produced from  $\text{CO}_2$  by an indium cathode. Similarly, an indium electrocatalyst converting  $\text{CO}_2$  to formate was recently used in combination with pure cultures of *Escherichia coli* strains, genetically engineered to enable the production of pyruvate from formate and  $\text{CO}_2$ .<sup>[15]</sup>

These studies gave evidence on a syntrophic relationship between the microorganisms and the metal catalyst. However, it was not shown whether this relationship was beneficial for both catalyst (i.e. mutualistic), or only benefitted the microbial catalyst, while not affecting (i.e. commensalistic) or even negatively affecting (i.e. parasitic) the performance of the metal catalyst. Tailoring the experimental conditions, such as the electrolyte composition, to the requirements of one catalyst, can lead to deviation from the optimal conditions for the second catalyst, and consequently decrease its performance.  $\text{CO}_2$  conversion with metals electrocatalysts is commonly performed within simple electrolyte media, and currently more research is ongoing to study the effect of additives, such as nutrients contained in microbial growth medium. While the effect of added nutrients on the Indium catalyst was not previously reported,<sup>[14,15]</sup> more recent studies on similar indium electrodes reveal a significant decrease in the production rate and coulombic efficiency towards formate, during electrochemical  $\text{CO}_2$  reduction in microbial medium electrolyte.<sup>[7b]</sup> Catalytic co-operation in the same reactor vessel may be therefore limited by the negative effect of microbial growth conditions on the electrocatalyst (i.e. parasitic relationship).

A sequential reaction approach for catalytic co-operation offers the possibility to optimize the electrolyte for each catalytic process. As such, a two-step process has been recently demonstrated based on silver catalyst for the electrocatalytic conversion of  $\text{CO}_2$  to syngas, which was subsequently converted to butanol and hexanol in a microbial fermentation chamber by a mixed culture of *Clostridium autoethanogenum* and *C. kluyveri*.<sup>[16]</sup> Similarly, a two-step system for co-catalytic  $\text{CO}_2$  reduction using formate as an intermediate has also been proposed, based on a three-chamber electrochemical reactor. In this approach, formate was abiotically produced by a tin electrocatalyst in the cathode chamber, and was subsequently transferred to the adjacent chamber via electrodialysis, where it was converted to methane by a pure culture of *Methanococcus maripaludis*.<sup>[17]</sup> However, accumulation of formate in the cathode chamber during operation resulted in kinetic limitations and decrease in formate production rate.<sup>[17]</sup> Direct consumption of the produced formate from the same electrolyte would alleviate the need for high formate concentration to create a gradient and energy needed for an efficient extraction.

The selection of both the metal and the microbial catalysts is expected to affect the overall applicability and feasibility of such co-catalytic processes. A plethora of catalysts have been proposed for the electrocatalytic reduction of  $\text{CO}_2$ , based on precious, scarce and expensive metals such as platinum, gold, silver, indium and tin, as well as more abundant, inexpensive catalysts, such as iron, copper or zinc.<sup>[2c]</sup> From an application perspective, the use of the later shows more relevance, due to the lower costs and availability.<sup>[18]</sup> Copper is unique among metal catalysts, as it has been shown to catalyze  $\text{CO}_2$  conversion to multiple products, including carbon monoxide, methane and formate, as well as multi-carbon compounds, such as ethylene and ethanol.<sup>[19]</sup> In terms of the bio-catalyst, the use of wild-type, mixed microbial cultures would facilitate the application in open-culture technologies. An additional advantage of using a mixed consortium of wild-type organisms as bio-catalysts is the latent adaptation capacity of the microbial community to potentially inhibiting compounds that could be derived from the electrode itself via leaching<sup>[20]</sup> or from (some of) the formed electro-synthesized compounds, such as reactive oxygen species.<sup>[14,15]</sup> Using a widely available metal like copper and combining it with wild type mixed microbial cultures would bring a new venture to work towards (more) applicable and sustainable integrated microbial electrochemical technologies.

The objective of the present research is to explore the potential for a syntrophic relationship between a non-precious CO<sub>2</sub>-reducing electrocatalyst (copper oxide, CuOx) and a bio-catalyst (wild-type mixed microbial culture), whereby formate is the intermediate product. To our knowledge, this is the first study to test catalytic cooperation using copper electrodes and mixed microbial cultures. A two-step approach was selected, to electrocatalytically produce formate in a microbial medium, which was consequently evaluated for microbial utilization. First, a series of different CuOx catalyst electrodes were studied with respect to the role of surface morphology, attachment and stability of the CuOx catalytic layer on the electrode, Cu-ion leaching, and formate formation under long-term operation (up to 4 days, longer than typical electrocatalysis experiments with duration of a few hours). The best catalyst was selected for further experiments. As the focus of this research is to recover liquid products of CO<sub>2</sub> electro-reduction, gas product formation was not monitored. To elucidate the effect of microbial growth conditions (i.e. electrolyte composition) on the metal catalyst, the electrochemical performance of CuOx electrodes was tested in the presence and absence of microbial growth medium. Finally, to evaluate the feasibility of sequential catalytic formate production and utilization, a CuOx electrode was used to produce formate, and the complete electrolyte was used as medium for wild type micro-organisms.

Contrary to previous findings,<sup>[7b]</sup> we show that microbial growth-medium electrolyte not only allows the electrocatalytic conversion of CO<sub>2</sub> to formate, but in fact enhances the catalytic activity of the CuOx electrodes, during abiotic electrochemical tests at low overpotential (−0.59 V vs RHE). Microbial growth conditions (i.e. growth medium electrolyte composition) can therefore have a positive effect on the performance of the metal catalysts under the conditions tested here. Microorganisms readily consumed the electrocatalytically produced formate from the effluent of a CuOx abiotic electrochemical reactor, which was amended with additional hydrogen and CO<sub>2</sub>, leading to microbial growth, as well as acetate and methane production. Overall, these results show potential for integrating mutualistic syntrophic CO<sub>2</sub> reduction processes of electrocatalysts and bio-catalysts, to form chain-elongated multi-carbon fatty acids from CO<sub>2</sub> in microbial electrochemical technologies.

## 2. Results and Discussion

### 2.1. CuOx electrode development: catalyst stability and activity are inversely related

It has been previously shown that the annealing duration and temperature can affect the resulting structure and consequently the catalytic activity of CuOx electrodes.<sup>[21]</sup> Accordingly, different annealing conditions were tested here, as summarized in Table 3 (in Materials & Methods), and photographs of the resulting electrodes are shown in Figure 1. Electro-polished Cu-foil (Figure 1a) had a shiny metallic texture and brown color. After annealing, a dark-colored layer of rough texture devel-

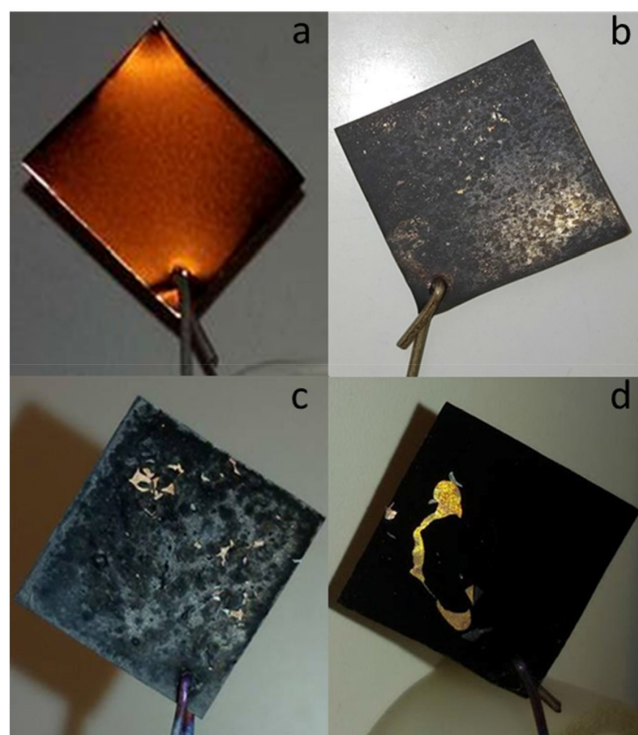


**Figure 1.** Copper electrodes tested in this study. a: electropolished; b: CuOx300: annealed at 300 °C for 12 hours; c: CuOx500\_1: annealed at 500 °C for 1 hour; d: CuOx500\_2: annealed at 500 °C for 2 hours.

(Figure 1b–d). On some of the annealed electrodes (Figure 1c–d), cracks were evident on the dark CuOx layer, revealing the metallic yellow/brown copper foil underneath. This indicates that the adhesion and homogeneity of the copper oxide layer was not the same among annealing treatments. Annealing at 500 °C for 12 hours, as has been previously performed,<sup>[21]</sup> resulted in complete detachment of the oxide layer from the electrode surface (not shown). To improve the stability of the catalyst, a lower annealing temperature (300 °C for 12 hours), as well as lower temperature ramp and shortened annealing durations at 500 °C, were tested. Decreasing the duration at 500 °C improved the stability of the oxide layer, leading to a more homogeneous but less stable coverage after 2 hours (Figure 1d), compared to 1 hour of annealing (Figure 1c). Among the conditions tested, annealing at 300 °C for 12 hours resulted in the most stable adhesion of the oxide layer (Figure 1b), as is evident by visual inspection of the resulting electrodes.

A typical example of the current density (i.e. electron flow rate per catalyst surface area) recorded over time during electrochemical experiments with a CuOx catalyst is shown in Figure 2a. A negative sign is typically assigned to the current when studying cathodic processes; more negative values indicate higher current. Within the first minutes, the current density changed rapidly from less than  $-4.2 \text{ mA cm}^{-2}$  to about  $-3.3 \text{ mA cm}^{-2}$ . Sharp decrease in the current density during the first minutes has been previously attributed to the reduction of the oxide layer that occurs upon applying a negative cathode

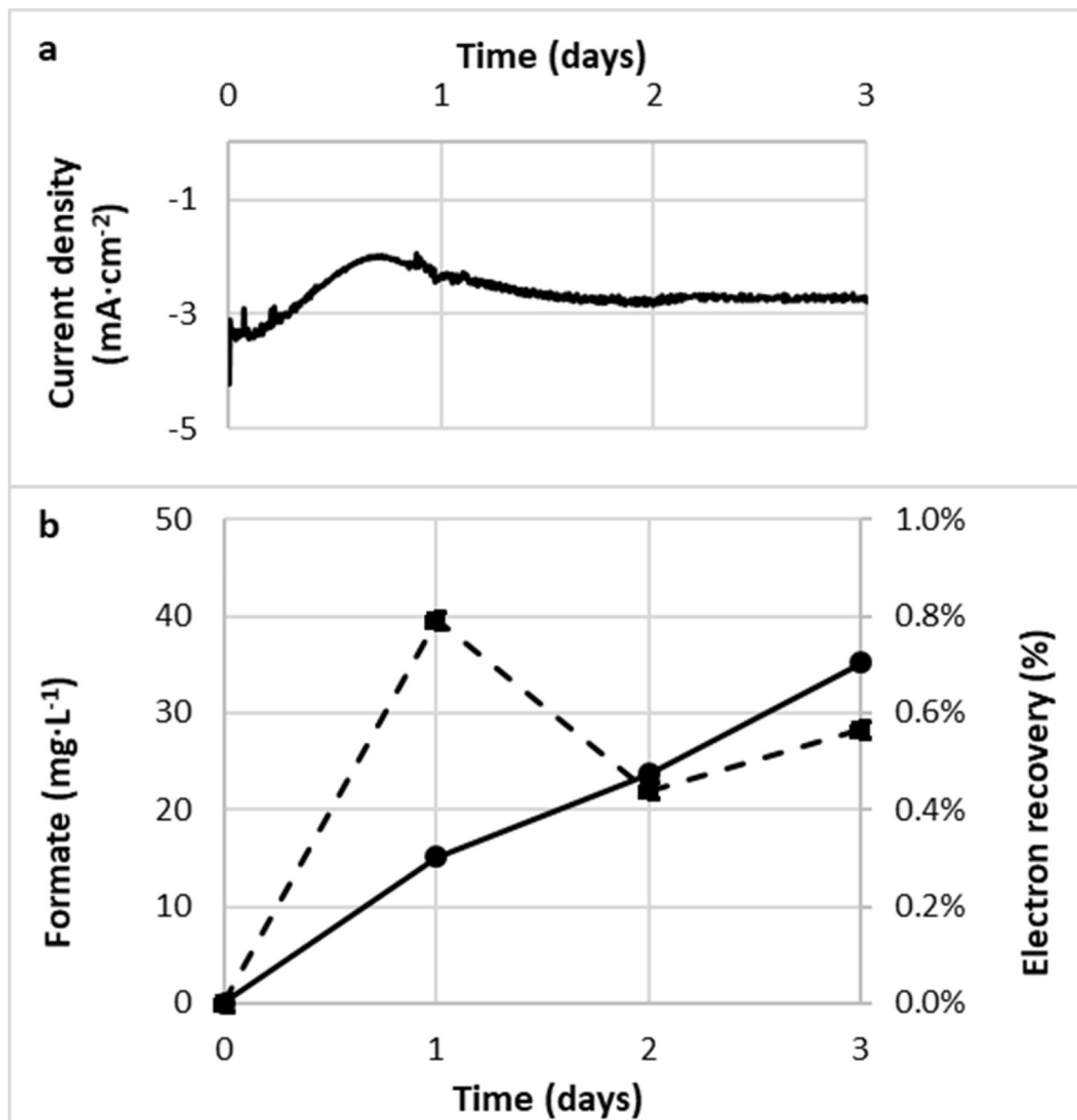


**Figure 2.** Electrocatalytic formate production with CuOx300 electrode at  $-0.59$  V under continuous  $\text{CO}_2$  supply. Above: Recorded current density over time. Below: formate concentration (solid line, left axis, in  $\text{mg}\cdot\text{L}^{-1}$ ) and calculated electron recovery (dashed line, right axis, in %) over time.

potential on the metal oxide cathode.<sup>[21]</sup> Please note that an interval time of 5 minutes was used to collect data for current. The actual initial value of the current during the first 5 minutes of the experiments was therefore unknown. Current density slowly decreased to  $-2\text{ mA}\cdot\text{cm}^{-2}$  and thereafter increased to about  $-3\text{ mA}\cdot\text{cm}^{-2}$  within the first two days, before reaching a stable value of  $-2.7\text{ mA}\cdot\text{cm}^{-2}$  until the end of the experiment (Figure 2a). Reduction of oxidized compounds in the electrolyte and on the electrode occurs at variable rates and resulted in this distinct pattern of current flow, before a steady-state was reached.

The concentration of formate product in the liquid phase during the electrochemical experiment, and the corresponding

electron recovery (i.e. percentage of electrons recovered in formate) are reported in Figure 2b (left and right axis, respectively). Formate concentration increased over time in the electrolyte (solid line, Figure 2b), indicating continuous production. Instead, electron recovery to formate (dashed line, Figure 2b) decreased from 0.8% on day 1 to less than 0.6% on days 2 and 3. Decrease in electron recovery over time was observed with all catalysts tested in microbial growth medium electrolyte. Similar decrease is often reported for electrochemical experiments in buffer electrolytes, and is attributed to catalyst poisoning.<sup>[22]</sup>

The electrochemical performance of CuOx electrodes annealed at different conditions, as well as of electro-polished Cu-



foil electrode (control), is summarized in Table 1. Gas products were not characterized, and thus a comparison among the catalyst can only be performed in terms of current density and formate production. All CuOx catalysts tested here were able to catalyze CO<sub>2</sub> reduction to formate in microbial medium electrolyte, whereas no formate production was detected with the Cu-foil electrode (Table 1, row 4). The recorded current density was approximately  $-2.2 \pm 0.09 \text{ mA cm}^{-2}$  for all electrodes tested (Table 1, column 2), and was therefore not affected by the annealing conditions. Among the CuOx catalysts, formate production rate increased with increasing annealing temperatures and duration (Table 1, column 4), from  $12 \text{ mg L}^{-1} \text{ day}^{-1}$  (CuOx300) to  $85 \text{ mg L}^{-1} \text{ day}^{-1}$  (CuOx500\_2). The calculated electron recovery to formate (Table 1, column 3) follows the same trend and increases from 0.8% (CuOx300) to 4% (CuOx500\_2). Therefore, the selectivity for formate production in microbial medium electrolyte increases with increasing annealing temperature (from 300 °C to 500 °C) and duration (from 1 to 2 hours at 500 °C), as has been previously shown for CuOx electrodes in bicarbonate electrolyte.<sup>[21]</sup>

For electrodes annealed at 500 °C, it was observed that part of the surface oxide layer detached from the electrode upon contact with the electrolyte. No further changes could be observed on the electrode surface during immersion in the electrolyte and CO<sub>2</sub> flushing for 30 minutes. After applying a negative cathode potential, cracks rapidly appeared on the copper oxide surface, as it became reduced, resulting in more detachment of the oxide layer. Please note that, unlike in heterogeneous catalysis, detached and/or leached species are less likely to be active, because the electrons, essential for the reaction, are only available on the electrodes. While the formate production rate after 48 hours with CuOx300 was the lowest among the CuOx electrodes tested (Table 1, column 4), this catalyst exhibited the highest robustness and adhesion of the catalyst layer. Therefore, CuOx300 catalyst was selected for further experiments, the results of which are presented below.

## 2.2. The effect of electrolyte on CO<sub>2</sub> reduction with CuOx electrocatalyst

CO<sub>2</sub> electro-reduction has been typically performed using a bicarbonate-based electrolyte.<sup>[23]</sup> In contrast, when using micro-organisms, the electrolyte has a different composition, mainly

phosphates (Na<sub>2</sub>HPO<sub>4</sub> – KH<sub>2</sub>PO<sub>4</sub> buffer), growth nutrients and trace metal elements. As the first requirement for co-catalytic cooperation, we have shown that CuOx catalysts are able to produce formate in microbial growth medium electrolyte (Table 1). To clarify the implications and bottlenecks of catalytic co-operation, the effect of the microbial medium electrolyte on the catalyst's activity was further evaluated. Aside from bicarbonate buffer (0.1 M KHCO<sub>3</sub>), phosphate buffer (6 g L<sup>-1</sup> Na<sub>2</sub>HPO<sub>4</sub>, 3 g L<sup>-1</sup> KH<sub>2</sub>PO<sub>4</sub>) was also compared with growth medium, to better understand the effects of the added nutrients and trace elements. Among replicates, one representative experiment was selected for further characterization of used catalysts with SEM-EDX, and the results of this representative experiment are reported in the rest of section 2.

### 2.2.1. Electrolyte composition affects the electrode surface structure and composition

To elucidate the effects of electrolyte composition on the micro-scale structure and surface composition of used CuOx300 electrodes, SEM-EDX was performed before and after electrochemical testing in biological growth medium and buffer electrolytes, and the results are summarized in Figure 3 and Table S1 (Supporting Information). The relative amount of oxygen detected on the electrode decreased from 14.6% to approximately 4% after testing in all electrolytes, accompanied by an equivalent increase in the amount of copper, suggesting that reduction of the copper oxide surface took place during electrochemical tests. Iron, phosphorus and potassium could be detected on used electrodes, indicating that deposition of some elements may take place on the electrode during operation. Unused CuOx300 electrode was mostly homogeneously covered with copper nanostructures (Figure 3a), although some cracks were present on the oxide layer (Figure 3e), as is also evident by visual observation of the electrode (Figure 1b). After electrochemical testing in all electrolytes, more micro-scale cracks appeared on the surface (Figure 3d, f, h). Similar cracks have been previously observed on the electrode surface of thick CuOx films, after electrochemical testing in 0.1 M KHCO<sub>3</sub> at  $-0.99 \text{ V}$ , likely caused by volume changes during rapid reduction of the CuOx film.<sup>[5f]</sup> Smaller, more abundant cracks were formed on the catalytic surface after operation in biological growth medium (Figure 3h), compared to simple buffer electrolytes (Figure 3d, f). Overall, these results indicate that the structure of the catalyst during electrochemical operation is affected by the electrolyte composition. Variation in the structure could affect the catalyst activity in different electrolytes, as is further discussed in section 2.4.

### 2.2.2. Electrolyte variations alter the current flow during CO<sub>2</sub> electro-reduction

Aside from the catalyst structure, the electrolyte composition can affect the electrochemical performance, for example due to pH, conductivity and substrate availability differences. To get

**Table 1.** Summary of electrochemical results with different CuOx catalysts, at  $-0.59 \text{ V}$  for 72 hours, in CO<sub>2</sub>-flushed biological growth medium electrolyte (pH 6.7). The  $\pm$  indicates standard deviation among experimental repetitions.

Catalyst	Average current density [ $\text{mA cm}^{-2}$ ] between 48–72 hours	Formate electron recovery after 72 hours [%]	Formate production rate after 72 hours [ $\text{mg L}^{-1} \text{ day}^{-1}$ ]
CuOx300	$-2.26 \pm 0.64$	$0.8 \pm 0.08$	$12.3 \pm 0.8$
CuOx500_1	$-2.25 \pm 0.20$	$2.0 \pm 0.5$	$47.0 \pm 6.1$
CuOx500_2	$-2.06 \pm 0.12$	$4.0 \pm 0.3$	$85.3 \pm 19.4$
Cu-foil (control)	$-2.23 \pm 0.55$	$0 \pm 0.0$	$0 \pm 0.0$

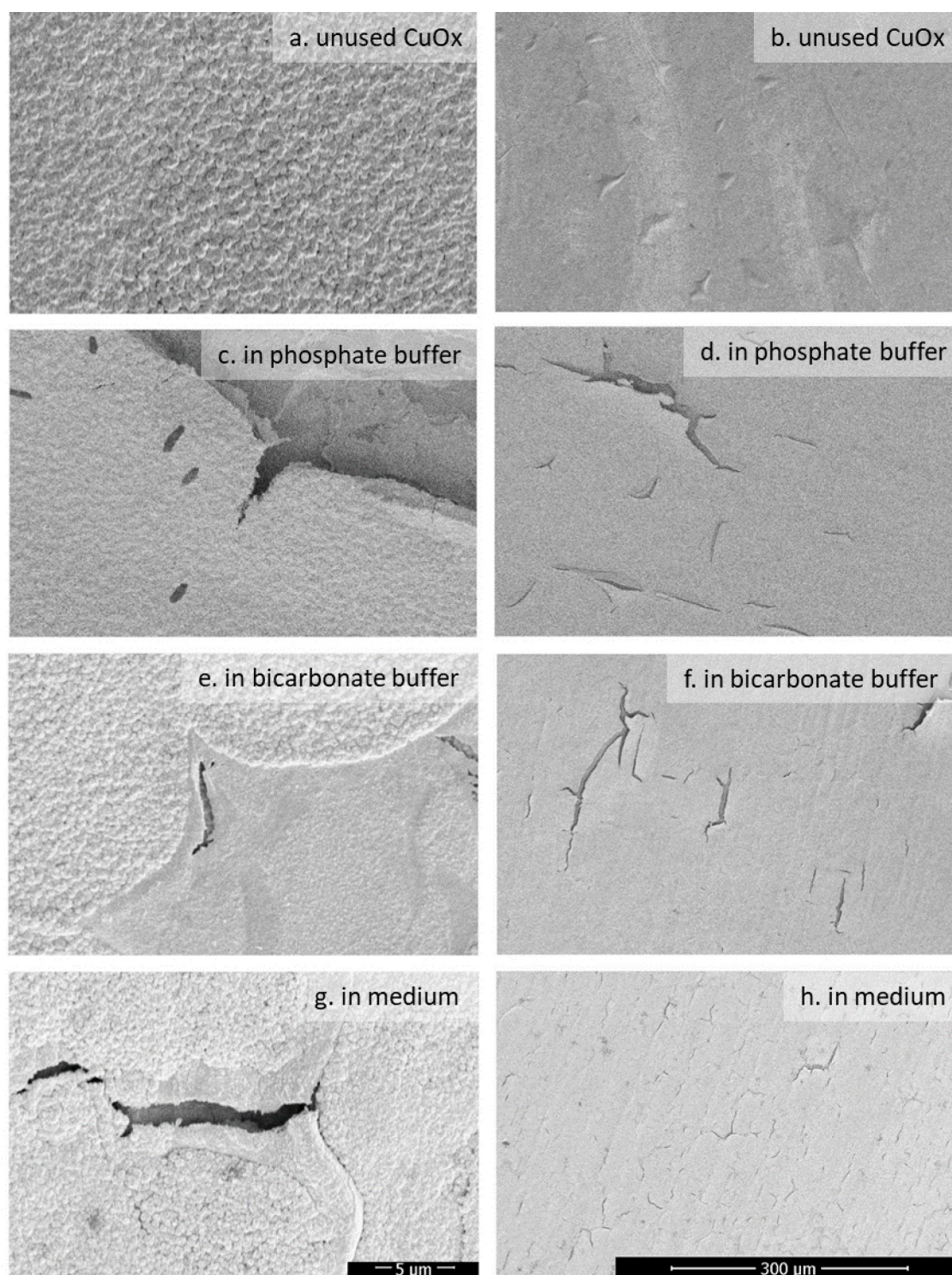


**Figure 3.** SEM images at two different scales (a, c, e, f at 5  $\mu\text{m}$  and b, d, f, h at 300  $\mu\text{m}$ ) of CuOx300 electrodes before (a, b) and after use for 3 days in electrochemical tests in phosphate buffer (c, d), bicarbonate buffer (e, f) and microbial growth medium electrolyte (g, h).

this insight, the electrocatalytic activity of CuOx300 electrodes was tested in different electrolytes, and the results are reported in Figure 4 and Table 2.

The pattern of current flow in the three electrolytes is shown in Figure 4a and b. For all electrolytes, the current was

initially more negative (e.g. less than  $-3 \text{ mA cm}^{-2}$  in bicarbonate), but within the first 10 minutes, it sharply decreased to less negative values (e.g. less than  $-1 \text{ mA cm}^{-2}$  for bicarbonate, Figure 4a). Thereafter, different trends emerged in the current flow for each electrolyte (Figure 4b). The current density

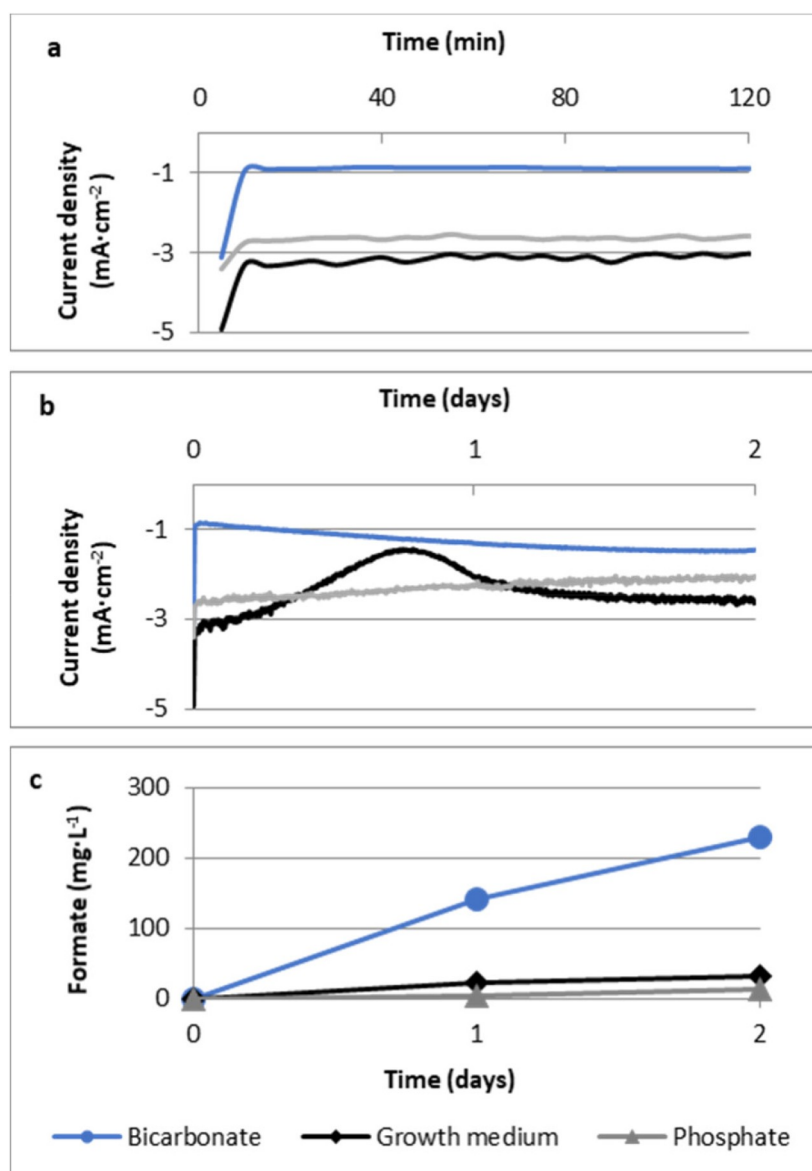


**Figure 4.** Electrocatalytic formate production with CuOx300 at -0.59 V under continuous CO<sub>2</sub> supply in various electrolytes. a, b: Recorded current density over time. Data from the first two hours of operation are shown in more detail (a). c: formate concentration in different electrolytes over time.

**Table 2.** Summary of electrochemical results with CuOx300 in biological growth medium, phosphate buffer (6 g L<sup>-1</sup> Na<sub>2</sub>HPO<sub>4</sub>, 3 g L<sup>-1</sup> KH<sub>2</sub>PO<sub>4</sub>) and bicarbonate buffer (0.1 M KHCO<sub>3</sub>) electrolytes. All experiments were performed at -0.59 V for 48 hours, in CO<sub>2</sub>-flushed electrolyte. For comparison, the concentration of Cu<sup>2+</sup> in the growth medium was 7.6 μg L<sup>-1</sup>, whereas no trace metals were present in buffer electrolytes.

Electrolyte	Bicarbonate buffer	Phosphate buffer	Growth medium
Formate production rate (mg L <sup>-1</sup> day <sup>-1</sup> )	115	6.15	15.8
48 hours formate electron recovery (%)	12%	0.36%	0.9%
Initial [Cu <sup>2+</sup> ] in solution (μg L <sup>-1</sup> )	190	240	281
[Cu <sup>2+</sup> ] in solution after 48 hours (μg L <sup>-1</sup> )	14	< 10	28.5
pH range	7.1–7.4	6.6–6.7	6.6–6.7
Conductivity (mS cm <sup>-2</sup> )	9.80	7.70	8.40

became progressively more negative in bicarbonate buffer, whereas the opposite was observed in phosphate buffer. Compared to buffer electrolytes, growth medium electrolyte resulted in a more complex pattern for current evolution (Figure 4b). During the first 10 minutes, current was more negative in this electrolyte. Within the first 24 hours, it slowly decreased and thereafter increased to more negative values again, reaching a steady current of about -2.5 mA cm<sup>-2</sup>, more negative than with either buffer electrolyte.

The sharp decrease in current observed in all electrolytes during the first 10 minutes of the experiment (Figure 4a) was likely due to the initial reduction of the oxide layer. Some of the differences observed in current flow over time could be due to the different pH among electrolytes, shown in Table 2 (row 6). In bicarbonate buffer, the pH decreased from 7.4 to 7.1 within



48 hours, whereas phosphate-based electrolytes had a steady pH of 6.6–6.7 throughout the experiment. Electron-consuming reactions such as  $H_2$  evolution can be pH-dependent,<sup>[24]</sup> and therefore difference in pH could explain the difference in current evolution over time between the two buffer electrolytes. Compared to phosphate buffer, added nutrients and trace elements in the growth medium did not affect the pH (6.6–6.7 for both electrolytes). However, some components may get reduced or electrodeposited on the electrode surface, such as iron, which was detected on the electrode surface after operation in microbial growth medium (Table S1). Therefore, other components in the medium aside from  $CO_2$  substrate may act as electron sinks, leading to increased current flow.

Copper itself can act as an electron sink during cathodic operation, thereby affecting the current flow. Table 2 shows the initial (row 4) and final concentration (row 5) of dissolved  $Cu^{2+}$  ions in each electrolyte during this experiment. The initial  $Cu^{2+}$  ion concentration in solution for every electrode was measured after 30 minutes of contact with the electrolyte and  $CO_2$  flushing, before applying a negative cathode potential. In all electrolytes, the initial concentration of dissolved  $Cu^{2+}$  in solution increased from  $0 \mu g L^{-1}$  (compared to fresh buffer) or from  $7.6 \mu g L^{-1}$  (compared to fresh growth medium) to higher than  $100 \mu g L^{-1}$ , indicating leaching. Decreasing concentration in all electrolytes over the course of the experiment reveals that  $Cu^{2+}$  ions deposit on the electrode during cathodic operation. EDTA, present in the growth medium, has a strong binding affinity and readily forms complexes with dissolved  $Cu^{2+}$  ions.<sup>[25]</sup> EDTA may therefore explain the delay in achieving a steady current observed with growth medium electrolyte, compared to simple buffer electrolytes. Dissolved  $Cu^{2+}$  concentrations among different electrolytes confirm that  $Cu^{2+}$  reduction/redeposition is affected by the electrolyte composition (Table 2). Compared to buffer electrolytes, more  $Cu^{2+}$  was leached in solution at the start of the experiment in growth medium electrolyte (Table 2, row 4). Detectable amounts of dissolved  $Cu^{2+}$  in growth medium electrolyte indicate that  $Cu^{2+}$  reduction was not complete after 48 hours, compared to simple buffer electrolytes (Table 2, row 5). EDTA present in the growth medium may be responsible for the observed (re-)solubilization of  $Cu^{2+}$ . Likely, continuous solubilization and re-deposition of copper occurred during electrochemical experiments in microbial growth medium electrolyte, due to the opposing forces of EDTA and negative cathode potential.

### 2.2.3. Bicarbonate buffer enhances formate production at low overpotential

The concentration of produced formate in the liquid phase during experiments with different electrolytes is shown in Figure 4c. The product concentration by the end of the experiment was higher in bicarbonate buffer ( $230 mg L^{-1}$ ) compared to phosphate-based electrolytes (less than  $32 mg L^{-1}$ ). The highest electron recovery to formate (12%) was calculated in bicarbonate buffer after 48 hours, followed by growth medium and phosphate buffer (Table 2, row 3). Since no liquid product

other than formate was detected, gaseous products (e.g.  $H_2$ ,  $CH_4$  or  $CO$ ) likely accounted for the remaining electrons. Aside from formate, under similar conditions, Kas and co-workers<sup>[26]</sup> reported an electron recovery of approximately 54% for  $CO$  and 17% for  $H_2$  evolution, using copper foam electrodes at  $-0.55 V$  in  $0.3 M KHCO_3$ . Ren and co-workers<sup>[5f]</sup> tested  $CuOx$  electrodes at  $-0.6 V$  and reported the formation of  $H_2$ ,  $CO$  and ethylene with electron recovery of approximately 70%, 25% and 5%, respectively, in  $0.1 M KHCO_3$ . Kuhl and co-workers<sup>[27]</sup> also reported  $H_2$  as the main product (approximately 75%), followed by 18%  $CO$ , and 9% formate. In the present work, gas bubble formation was observed by eye on the electrode surface during electrochemical experiments, which supports that gaseous products were produced, acting as an alternative electron sink.

As gas composition was not analyzed during these experiments, a complete comparison of the electrocatalytic activity of  $CuOx300$  among different electrolytes and with previously reported results for copper electrodes is not possible. Nevertheless, within the first 24 hours, an electron recovery of 17% to formate was calculated in bicarbonate buffer (not shown in Table 2), which is comparable with previously reported results under similar conditions. For example, electron recovery of 24% to formate has been reported for  $CuOx$  electrodes annealed at  $300^\circ C$  for 5 hours, operating for 7 hours at  $-0.5 V$  in  $0.5 M NaHCO_3$  buffer.<sup>[21]</sup> It should be noted that a time interval of 24 hours was selected here, compared to shorter sampling intervals used in literature (e.g. 1 hour). Given that electrocatalytic activity decreases over time,<sup>[22]</sup> longer interval times may result in underestimation of the electron recovery reported here, compared to other studies.

Enhanced productivity in bicarbonate buffer compared to the phosphate-based electrolytes could be due to higher substrate availability (i.e. dissolved  $CO_2$ ), as a result of the pH.  $CO_2$  solubility increases with increasing pH, and therefore higher pH in bicarbonate electrolyte (7.1–7.4), compared to phosphate-based electrolytes (6.6–6.7, Table 2, row 6), could explain the increased formate production in the former. However, increased formate production in bicarbonate buffer cannot be solely attributed to the pH differences. For example, Ren and co-workers<sup>[5f]</sup> tested  $Cu$ -foil electrodes at  $-0.99 V$ , and reported higher electron recovery into formate in  $0.1 M KHCO_3$  buffer (12.7%), compared to phosphate buffer electrolyte (5.6%,  $0.1 M K_2HPO_4 - KH_2PO_4$ ). Instead, the electron recovery into  $H_2$  was enhanced in the phosphate buffer electrolyte (95%, compared to 50% in bicarbonate).<sup>[5f]</sup> The difference in bulk pH after  $CO_2$  flushing was only minor among the two electrolytes (6.79 for bicarbonate and 6.73 for phosphate buffer),<sup>[5f]</sup> and therefore other factors should be considered to explain the enhanced formate production in bicarbonate electrolyte.

One explanation for the increased formate production in bicarbonate electrolytes could be the mechanism of electrocatalytic formate production at low over-potentials. Kortlever and co-workers<sup>[28]</sup> used  $Pd$  electrocatalysts for the reduction of  $CO_2$  and reported different reaction mechanisms at low over-potentials compared to more negative cathode potentials. Comparing the activity over different potentials, two peaks were distinguished, the first at approximately  $-0.4 V$ , and the

second below  $-1$  V. The authors attributed this behavior to direct bicarbonate reduction at low-overpotentials, a different reaction mechanism than the direct  $\text{CO}_2$  reduction occurring at high overpotentials. Formate production was also recorded in  $0.5$  M  $\text{KHCO}_3$  buffer at pH of  $8.4$ , without additional  $\text{CO}_2$  flushing, supporting that direct bicarbonate reduction occurs at low overpotential.<sup>[28]</sup> A similar mechanism has also been proposed for copper electrocatalysts in  $1$  M  $\text{KHCO}_3$  electrolyte, with a reduction peak for direct bicarbonate conversion at approximately  $-0.6/-0.7$  V.<sup>[23]</sup> It is therefore likely that direct reduction of bicarbonate to formate occurred at  $-0.59$  V tested in the present study. This could explain the increased electron recovery observed in bicarbonate electrolyte, as the substrate availability (i.e.  $\text{HCO}_3^-$ ) was higher than in phosphate buffer.

#### 2.2.4. Microbial growth components in phosphate buffer improve catalytic activity of CuOx

Various compounds in the microbial growth medium may have caused improving or relaxing activity of the CuOx catalyst. Growth medium contained the same components as phosphate buffer ( $\text{Na}_2\text{HPO}_4 - \text{KH}_2\text{PO}_4$ ), but included in addition EDTA, growth nutrients ( $\text{NH}_4^+$ ,  $\text{Cl}^-$ ,  $\text{Mg}^{2+}$ ,  $\text{Ca}^{2+}$ ), and trace elements (ions of Fe, B, Cu, I, Mn, Mo, Zn, Co, Ni). In both electrolytes, the electron recovery to formate was less than  $1\%$ , much lower compared to bicarbonate buffer ( $12\%$  after  $48$  hours). In spite of the low overall electron recovery, microbial growth medium electrolyte resulted in a significant increase of production rate and electron recovery to formate compared to plain phosphate buffer (Table 2), as was confirmed with repeated measurements.

The improvement in catalytic activity observed in microbial medium electrolyte, compared to phosphate buffer, cannot be specifically correlated with trace metals. Nevertheless, the present results contradict earlier reports on the effect of metal impurities. For example, trace amounts of iron have been shown to decrease the coulombic efficiency of  $\text{CO}_2$  conversion with Indium cathodes, due to deposition of iron on the electrode surface, which can thereafter catalyze  $\text{H}_2$  evolution.<sup>[29]</sup> A similar decrease in coulombic efficiency of Indium catalysts for  $\text{CO}_2$  electro-reduction to formate in the presence of mixed trace elements in the electrolyte has been recently reported.<sup>[7b]</sup> Deactivation of tin electrodes for  $\text{CO}_2$  electro-reduction to formate has been linked to deposition of metal impurities, primarily zinc.<sup>[22a]</sup> Cu electrocatalysts for  $\text{CO}_2$  reduction are also prone to poisoning by metal impurities, particularly iron and zinc.<sup>[30]</sup> One explanation for the observed differences could be that EDTA was present in the microbial growth medium used here, compared to previous studies, that did not include chelating agents in the electrolyte. EDTA has been recently shown to improve  $\text{CO}_2$  reduction with copper electrodes, by binding impurity metals, such as iron, nickel and zinc, and preventing deposition on the copper electrode.<sup>[25]</sup> EDTA results in continuous leaching of copper from the electrode, which simultaneously gets re-deposited due to the negative cathode potential. This dynamic regeneration of the catalyst's surface

further prevents catalyst poisoning due to accumulation of byproducts.<sup>[25]</sup> Therefore, EDTA present in microbial growth medium may have counteracted the (potentially) inhibiting effects of trace metals, and resulted in improved catalytic activity observed in microbial growth medium, compared to buffer electrolyte.

To clarify the behavior of trace elements present in the medium, dissolved metal ions in solution were measured over time during electrochemical experiments (Figure S2, Supporting Information). Aside from copper, the concentration of iron and molybdenum ions decreased over time in solution, while other trace elements remained dissolved (Figure S2). This could imply that some metals get deposited on the CuOx surface during operation. Iron was detected with SEM-EDX on the electrode after operation in biological growth medium (Table S1), which further supports that iron was deposited on the electrode during electrochemical testing. No molybdenum was detected on the electrode surface with EDX, which could be due to the lower amount of metal deposited, compared to iron. Alternatively, molybdenum depletion from the electrolyte could be due to precipitation, instead of deposition on the electrode. As gas products were not measured, the effect of metal deposition on CuOx300 catalytic activity for  $\text{H}_2$  evolution remains to be revealed.

Cations such as  $\text{Mg}^{2+}$  and  $\text{Ca}^{2+}$  present in the medium have been shown to affect catalyst's activity, and could therefore be responsible for the observed differences between microbial medium and phosphate buffer. It has been previously shown that potassium iodine in phosphate buffer electrolyte can strongly adsorb on the electrode and promote  $\text{H}_2$  production over  $\text{CO}_2$  electro-reduction.<sup>[23]</sup> Lewis acid cations such as  $\text{Mg}^{2+}$  and  $\text{Ca}^{2+}$  have been previously shown to have a synergistic effect and improve  $\text{CO}_2$  electro-reduction with iron(0) tetraphenyl-porphyrins.<sup>[31]</sup> Cations such as  $\text{Na}^+$  have also been shown to improve the performance of anode electrocatalysts for glycerol oxidation, presumably via adsorption and interaction with the organic substrate, thus resulting in closer proximity to the electrocatalyst.<sup>[32]</sup> It has been hypothesized but not clearly shown that large cations can adsorb on the surface of copper electrodes, thus affecting the catalytic activity for  $\text{CO}_2$  reduction.<sup>[23]</sup> More recently, it was shown that cations such as  $\text{Li}^+$ ,  $\text{Na}^+$ ,  $\text{K}^+$ ,  $\text{Rb}^+$ , and  $\text{Cs}^+$  can affect the selectivity during CO electro-reduction on copper electrodes.<sup>[33]</sup> Using SEM-EDX, no  $\text{Mg}^{2+}$  and  $\text{Ca}^{2+}$  were detected on the electrode surface after use in microbial medium (Table S1), either due to lack of adsorption, or due to undetectable amounts adsorbed.  $\text{K}^+$  was detected on all electrodes at different concentrations, with higher amounts detected in the presence of bicarbonate buffer (Table S1), likely due to higher concentration of  $\text{K}^+$  in this electrolyte, compared to phosphate-based electrolytes. Interestingly,  $\text{Na}^+$  was detected on the surface after electrochemical testing in phosphate buffer, but not in growth medium (Table S1), although  $\text{Na}^+$  concentration in both electrolytes was the same. Different trends in cation adsorption among electrolytes could (partially) explain the differences in catalytic activity, but the exact mechanism cannot be further elucidated at this stage.

Aside from the elemental composition, the surface microstructure of CuOx electrodes may be responsible for the different performance among the tested electrolytes. Variations due to electrolyte composition were observed in the electrode microstructure after electrochemical testing (Figure 3). More abundant and smaller surface defects developed on the CuOx surface in microbial medium, compared to buffer electrolytes. Surface defects have been previously associated with increased catalytic activity of metal electrodes for CO<sub>2</sub> reduction.<sup>[26,34]</sup> Compared to metal nanoparticles, which can change in structure during operation (e.g. sintering), bulk defects could stabilize catalytically active structures that would otherwise be unstable under reaction conditions.<sup>[35]</sup> The improved catalytic activity observed in growth medium, compared to phosphate buffer electrolyte (Table 2), could be due to more abundant defects formed on the CuOx surface during electrochemical testing.

Overall, an improvement in the catalytic activity of CuOx300 is evident in the presence of complex growth medium, compared to simple phosphate buffer electrolyte.

### 2.3. Electrocatalytically produced formate is a suitable substrate for bio-catalysts

To investigate the metabolic cooperation between the catalysts, the two reactions were performed in sequence, using the effluent of the first reaction (formate production by metal catalyst) as influent for the second reaction (formate consumption by wild-type microorganisms). H<sub>2</sub> was added as additional electron donor and CO<sub>2</sub> as additional electron acceptor and carbon source, to ensure the availability of substrates for the homoacetogenic metabolic pathway.<sup>[8d]</sup> In order to perform the biological experiment in triplicate, while ensuring sufficient formate concentration in each bottle, electrocatalytic formate production with CuOx300 was performed for 96 hours at a more negative cathode potential (−1 V) than previously tested

(−0.59 V in Figure 4). The results of this experiment are presented in Supporting Information (Figure S3).

The concentration of substrates (i.e. CO<sub>2</sub>, H<sub>2</sub> and formate) and products (i.e. acetate) measured over time during biological experiments is shown in Figure 5. Liquid (right axis) and gaseous (left axis) substrate concentrations decreased over time, as can be observed for formate (black solid line), CO<sub>2</sub> (grey dashed line) and H<sub>2</sub> (black dashed line). Instead, product concentration increased over time, as can be observed for acetate (right axis, grey solid line). These results indicate that formate, H<sub>2</sub> and CO<sub>2</sub> were converted to acetate by the microorganisms. Trace amounts of methane product were also detected in all bottles (not shown in Figure 5).

An electron and carbon balance including all substrates and products measured is shown in Figure S4. The negative mass balance for both carbon and electrons in Figure S4 indicates that part of the substrate provided was consumed for other biological functions, besides product formation (e.g. cell growth), or incorporated in unidentified products. Based on the mass balances, it cannot be concluded whether formate was elongated to acetate by microorganisms, or used as a carbon and electron donor for other biological functions. Nevertheless, these results confirm that formate can be used as a metabolic intermediate between the CuOx electrocatalyst and bio-catalysts. No fresh medium was added to the serum bottles, therefore the effluent of the electrochemical reactor was the only source for nutrients and trace elements. Inhibition of biological activity due to the spent electrolyte was not quantified in the present study. Still, these results support that a metabolic cooperation is possible, as metal electrocatalyst operation did not lead to compete inhibition of microbial activity.

We have shown a proof-of-principle that metabolic cooperation between a copper electrocatalyst and a mixed microbial consortium is possible, using formate as an intermediate. For further optimization, more detailed studies on e.g. electrolyte composition are needed. For example, we have shown that

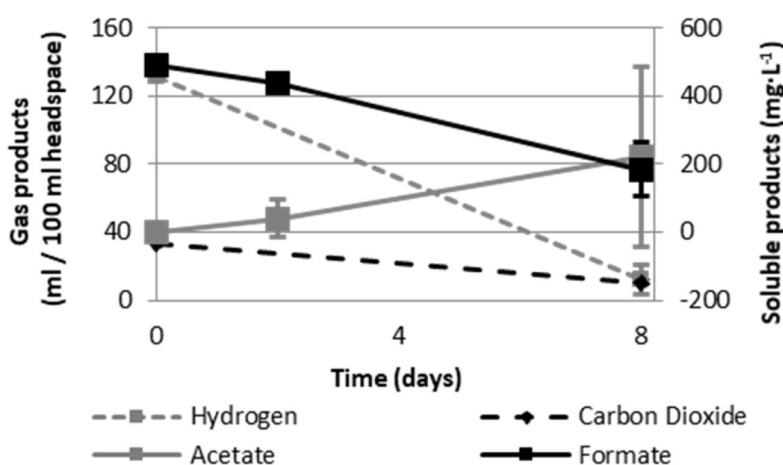


**Figure 5.** Hydrogen (black dashed line, left axis), carbon dioxide (grey dashed line, left axis), formate (black solid line, right axis) and acetate (grey solid line, right axis) concentrations in serum bottles over time. A mixture of H<sub>2</sub>:CO<sub>2</sub> (80:20) was added on day 0. Experiment was performed in triplicate; error bars represent the standard deviation.

EDTA contained in the growth medium likely resulted in an increase of formate selectivity for CuOx, compared to phosphate buffer. Aside from EDTA, which had a small but significant contribution to the electrocatalytic activity of CuOx, the major factor influencing the electron recovery to formate was the buffer composition, with much higher selectivities recorded in bicarbonate compared to phosphate-based electrolyte. Interestingly, microbial CO<sub>2</sub> conversion has been shown to proceed in a variety of growth media, which can contain high bicarbonate salt concentrations, comparable to the electrolyte composition used for CO<sub>2</sub> electro-reduction with metal catalysts. For example, Zaybak and co-workers used medium containing 0.1 M of NaHCO<sub>3</sub> and half the concentration of phosphate buffer compared to the present study, to cultivate a mixed culture of facultative anaerobic microorganisms for CO<sub>2</sub> conversion.<sup>[36]</sup> Similarly, Patil and co-workers used medium containing 0.24 M of NaHCO<sub>3</sub> and merely 0.2 g/L of K<sub>2</sub>HPO<sub>4</sub> as electrolyte for a mixed culture of microorganisms, converting CO<sub>2</sub> to acetate.<sup>[37]</sup> Nevertheless, the adaptability of the bio-catalyst to different medium compositions was outside the scope of this research.

Based on the results presented in this manuscript, combination of the two catalysts could be possible either in sequential reactors, or in the same reactor. The bio-catalyst could be potentially incorporated directly in the electrolyte of the electrochemical cell (i.e. planktonic growth) and/or on the cathode of the system (i.e. biofilm growth). This would allow a new microbial electrosynthesis technology, in which electrochemically produced formate may be directly utilized by microorganisms. Still, confirmation of this is required, as microbial activity may affect the electrocatalytic performance of the (CuOx) catalysts.

### 3. Conclusion

This is the first report of syntrophic catalytic cooperation between a CO<sub>2</sub>-reducing metal electrocatalyst and a mixed culture of naturally-occurring microorganisms (bio-catalysts), using formate as an intermediate product. Furthermore, this is the first study on co-catalytic CO<sub>2</sub> reduction to use copper; an inexpensive, versatile catalyst for CO<sub>2</sub> conversion to multiple products.

A copper electrocatalyst was able to produce formate under microbial growth conditions, albeit in low concentrations. A mixture of nutrients and trace elements, essential for biological growth, did not inhibit the catalytic activity of CuOx electrodes for formate production, as has been previously suggested. On the contrary, microbial growth medium enhanced formate production at low overpotentials in phosphate-based electrolyte.

Microbial conversion of formate to acetate and methane was possible, directly from the effluent of a formate-producing reactor with copper electrocatalyst. Effluent was used without treatment or addition of nutrients, and no inhibition of biological growth due to the electrochemical conditions applied was observed.

Taken together, these results provide support that a mutualistic syntrophic relationship between electrocatalysts and bio-catalysts may be possible in sequential reactions, or by integration of both catalyst in a single-stage microbial electro-synthesis process.

## Experimental Section

### Electrode preparation

Copper foil (Cu-foil), titanium and platinum wires were purchased from Salomon's Metalen B.V., the Netherlands. Cu-foil was cut in square pieces (2×2×0.01 cm), and each was connected to a titanium wire current collector (Ø=0.8 mm), by applying mechanical pressure to clamp the wire to the foil. To remove organic contaminants from the surface, electrodes were pre-treated by successive sonication in acetone (99.8%) for 30 min, followed by iso-propanol (99.95%) for 30 min and finally in demi water. Hereafter electrodes were electro-polished in concentrated phosphoric acid (85%) at a current of 2.08 A for one minute, with copper foil as the counter electrode. Finally, electrodes were rinsed with milli-Q water and dried under dry N<sub>2</sub> flow. The electro-polished Cu-foil electrodes were annealed in a muffle static air oven (Nabertherm P 330) at various temperatures and durations, to develop a surface copper(I) oxide layer, as has been previously described.<sup>[21]</sup> The different annealing conditions employed in this study are summarized in Table 3. Electrodes were manufactured in at least quadruplicates with a similar appearance. Adhesion of the oxide layer on the electrode surface was evaluated by visual inspection of annealed electrodes. For electrochemical experiments, anode (counter) electrodes were prepared by wrapping 7 cm of platinum wire (99.95% and Ø=0.3 mm) on the edge of a piece of titanium wire current collector. The reference electrode used for all electrochemical tests was Ag/AgCl (3 M KCl). All potentials in this paper were reported against the Reverse Hydrogen Electrode (RHE), calculated as:  $E \text{ (V vs. RHE)} = E \text{ (V vs. Ag/AgCl)} + 0.210 \text{ V} + 0.0591 \text{ V} \times \text{pH}$ .<sup>[21]</sup> An IVIUM n-stat potentiostat (IVIUM technologies B.V., the Netherlands) was used for all electrochemical techniques (material preparation and characterization).

### Catalyst Characterization

Surface characterization of the copper oxide catalyst was performed using Scanning electron microscopy (SEM, FEI Magellan 400 FESEM) with energy dispersive spectroscopy (EDS) (Oxford Instruments), before and after electrochemical tests.

### Electrochemical experiments

Chronoamperometry was performed in a 3-electrode mode using 2-compartment electrochemical H-type reactors, with a Nafion

**Table 3.** Annealing conditions for all copper oxide catalysts prepared for this study.

Catalyst abbreviation	Temperature ramp [°C min <sup>-1</sup> ]	Annealing Temperature [°C]	Annealing duration [hours]
CuOx300	3.06	300 °C	12 hours
CuOx500_1	2.71	500 °C	1 hour
CuOx500_2	2.71	500 °C	2 hours
CuOx500_12	2.71	500 °C	12 hours



cation-exchange membrane (projected surface area 11.3 cm<sup>2</sup>) separating the anode and cathode compartments. The anolyte (250 ml) was phosphate buffer, and the catholyte (220 ml) was autoclaved microbial growth medium. Bicarbonate buffer, as well as phosphate buffer, were used in the catholyte for some experiments (as indicated in the text), in order to compare the effect of different electrolytes on CO<sub>2</sub> electro-reduction with copper catalysts. The composition of all electrolytes used is shown in Table 4.

All electrochemical tests were performed at 25 °C. The catholyte was continuously flushed with pure CO<sub>2</sub> gas (50 ml min<sup>-1</sup>) during electrochemical experiments with mass flow controllers (Brooks Instruments). The headspace of the reactor was open to air via a water lock, allowing CO<sub>2</sub> and gas products to exit the reactor. Gas products were therefore not analyzed. All electrochemical experiments were performed in triplicate.

### Analysis of liquid samples

Gas chromatography (Agilent 7890B, USA) using flame ionization detection (GC–FID) was used to analyze liquid products from electrochemical experiments (C2–C8 volatile fatty acids and medium-chain fatty acids, C1–C6 alcohols). The concentration of formate was measured with high performance liquid chromatography (HPLC), with refractive index (RI) and UV detection (column specification: Aminex HPX-87H, 300 × 7.8 mm (BioRad 1225–0140). Inductively coupled plasma optical emission spectroscopy (ICP-OES) was used to quantify the amount of metal ions that leach from the cathode over time during electrochemical tests. The sampling frequency is varied among experiments (2–4 days).

### Biological Experiments

A bio-electrochemical reactor, which has been in operation for 3 years and contains a mixed wild-type microbial community, was used as source of microorganisms for the biological experiments reported here. Inoculum for this reactor was obtained from a previously-described bio-reactor.<sup>[38]</sup> Since the inoculation, microorganisms (i.e. bio-catalysts) in the reactor have been continuously producing acetate from CO<sub>2</sub>, at a cathode potential of –0.46 V, with a graphite felt (4 mm thick, CTG Carbon GmbH, Germany) cathode electrode. For the biological experiments shown here, microbial inoculum was prepared from a liquid sample of this reactor, twice centrifugated at 6000 rpm for 10 min and re-suspended in fresh

biological growth medium. The re-suspended pellets (microorganisms) were thereafter directly injected in vessels used for biological experiments.

Biological experiments were performed in serum bottles (125 ml total volume, 60 ml liquid volume), in the absence of electrodes. The medium used in these serum bottles was the effluent from an abiotic, electrochemical experiment with copper catalyst, used as received from the reactor (i.e. no filtration or adding chemicals). The effluent contained 487 mg L<sup>-1</sup> of formate, which was produced from CO<sub>2</sub> during electrochemical experiments by the metal catalyst. At the end of the electrochemical experiment, the electrode was removed from the reactor, and all the catholyte was collected. Under magnetic stirring and continuous CO<sub>2</sub> flushing in the liquid, three serum bottles were prepared, containing the same amount of effluent. During this time, less soluble gaseous products formed during the electrocatalysis (e.g. H<sub>2</sub>) were likely removed via CO<sub>2</sub> flushing. No liquid carbon-containing products except for formate was detected in the effluent, thus mainly formate was transferred as electron source for the microbial catalysts. After adding microbial inoculum, the medium in the serum bottles was flushed with gas (H<sub>2</sub>:CO<sub>2</sub> 80:20) for 30 min. The headspace volume was replaced with gas of the same composition, and was extended using a multi-layer foil gas bag (1 L capacity, purchased from Sense Trading, the Netherlands), containing 200 ml of the same gas mixture. To ensure the availability of electrons to drive the biological reaction, H<sub>2</sub> was added as an electron equivalent in this experiment, as no cathode potential was supplied. After the initial addition of gas at the start of the experiment, the gas phase was not further exchanged, and gas was not continuously supplied during this experiment, therefore gas products could be collected and analyzed, using gas chromatography, as previously described.<sup>[39]</sup> Dissolved gases in the liquid were not quantified. The experiment was performed in triplicate, under magnetic stirring at 25 °C. The consumption of formate and production of volatile fatty acids and methane in the serum bottles was followed for 8 days.

### Calculations

The current densities (in mA cm<sup>-2</sup>) reported throughout this manuscript were calculated based on the projected electrode surface area (2 sides of 4 cm<sup>2</sup> is in total 8 cm<sup>2</sup>).

For electrochemical experiments, electron recovery (%) was calculated between consecutive time points (i.e. with a time interval of 24 hours). The produced amount of formate (in mol) was calculated based on the concentration difference between sampling points, as measured with HPLC in liquid samples. The number of electrons (in mol) recovered in formate was estimated based on reaction stoichiometry (i.e. 2 mols of electrons per mol formate), and converted to electric charge, by multiplying with the Faraday constant (96485 C mol<sup>-1</sup>). Electron recovery was calculated as the percentage of electric charge recovered into formate, compared to the total electric charge between two sampling points, as recorded by the potentiostat.

Production rates (in mg L<sup>-1</sup> day<sup>-1</sup>) reported in this paper were calculated at the end of each batch experiment, by dividing the product concentration (in mg L<sup>-1</sup>) by the duration of the experiment (in days). It should be stressed that the reactors used were not optimized for high volumetric production rate, with an 8 cm<sup>2</sup> electrode per 220 mL catholyte. Changes in volume and dilution due to refreshing of the reaction medium were corrected for, when calculating the electron recoveries and production rates.

**Table 4.** Composition of electrolytes used in this study.

Component	Growth medium	Phosphate Buffer	Bicarbonate Buffer
KHCO <sub>3</sub>	–	–	10 g L <sup>-1</sup>
Na <sub>2</sub> HPO <sub>4</sub>	6 g L <sup>-1</sup>	6 g L <sup>-1</sup>	–
KH <sub>2</sub> PO <sub>4</sub>	3 g L <sup>-1</sup>	3 g L <sup>-1</sup>	–
NH <sub>4</sub> Cl	0.2 g L <sup>-1</sup>	–	–
MgCl <sub>2</sub> ·6H <sub>2</sub> O	0.04 g L <sup>-1</sup>	–	–
CaCl <sub>2</sub>	0.015 g L <sup>-1</sup>	–	–
FeCl <sub>3</sub> ·6H <sub>2</sub> O	1.5 mg L <sup>-1</sup>	–	–
H <sub>3</sub> BO <sub>3</sub>	0.15 mg L <sup>-1</sup>	–	–
CuSO <sub>4</sub> ·5H <sub>2</sub> O	0.03 mg L <sup>-1</sup>	–	–
KI	0.18 mg L <sup>-1</sup>	–	–
MnCl <sub>2</sub> ·4H <sub>2</sub> O	0.12 mg L <sup>-1</sup>	–	–
Na <sub>2</sub> MoO <sub>4</sub> ·2H <sub>2</sub> O	0.06 mg L <sup>-1</sup>	–	–
ZnSO <sub>4</sub> ·7H <sub>2</sub> O	0.12 mg L <sup>-1</sup>	–	–
CoCl <sub>2</sub> ·6H <sub>2</sub> O	0.15 mg L <sup>-1</sup>	–	–
NiCl <sub>2</sub> ·6H <sub>2</sub> O	0.023 mg L <sup>-1</sup>	–	–
ethylenediaminetetraacetic acid (EDTA)	10 mg L <sup>-1</sup>	–	–

## Acknowledgements

We gratefully acknowledge the Wageningen Institute for Environment and Climate Research (WIMEK), the Graduate School of Food Technology, Agrobiotechnology, Nutrition and Health Sciences (VLAg) of Wageningen University, as well as TKI Watertechnologie, Magneto special anodes B.V. and W&F Magneto B.V. for funding this work. We acknowledge the contribution of Virangni Soekhoe in performing preliminary experiments that helped shape the contents of this paper. We further acknowledge dr. Marcel Giesbers and Jelmer Vroom from Wageningen Electron Microscopy Centre for their valuable help during SEM-EDX analysis reported in this paper.

## Conflict of Interest

The authors declare no conflict of interest.

**Keywords:** bio-catalysis · carbon dioxide fixation · catalytic cooperation · formate electrosynthesis · supported catalysts

- [1] a) A. Demirbas, *Energy Sources Part B*, **2009**, *4*, 212–224; b) F. R. Pazheri, M. F. Othman, N. H. Malik, *Renewable Sustainable Energy Rev.*, **2014**, *31*, 835–845.
- [2] a) A. S. Agarwal, Y. Zhai, D. Hill, N. Sridhar, *ChemSusChem*, **2011**, *4*, 1301–1310; b) P. L. Tremblay, T. Zhang, *Front. Microbiol.*, **2015**, *6*, 201; c) J. Wu, Y. Huang, W. Ye, Y. Li, *Adv. Sci.*, **2017**, *4*, 1700194; d) F. Enzmann, M. Stöckl, A. P. Zeng, D. Holtmann, *Eng. Life Sci.*, **2019**, *19*, 121–132.
- [3] S. Verma, B. Kim, H. R. M. Jhong, S. Ma, P. J. A. Kenis, *ChemSusChem*, **2016**, *9*, 1972–1979.
- [4] a) J. L. Inglis, B. J. MacLean, M. T. Pryce, J. G. Vos, *Coord. Chem. Rev.*, **2012**, *256*, 2571–2600; b) O. Yishai, S. N. Lindner, J. Gonzalez de la Cruz, H. Tenenboim, A. Bar-Even, *Curr. Opin. Chem. Biol.*, **2016**, *35*, 1–9.
- [5] a) M. Le, M. Ren, Z. Zhang, P. T. Sprunger, R. L. Kurtz, J. C. Flake, *J. Electrochem. Soc.*, **2011**, *158*, E45–E49; b) R. Reske, M. Duca, M. Oezaslan, K. J. P. Schouten, M. T. M. Koper, P. Strasser, *J. Phys. Chem. Lett.*, **2013**, *4*, 2410–2413; c) F. Jia, X. Yu, L. Zhang, *J. Power Sources*, **2014**, *252*, 85–89; d) D. Chi, H. Yang, Y. Du, T. Lv, G. Sui, H. Wang, J. Lu, *RSC Adv.*, **2014**, *4*, 37329–37332; e) C. S. Chen, A. D. Handoko, J. H. Wan, L. Ma, D. Ren, B. S. Yeo, *Catal. Sci. Technol.*, **2015**, *5*, 161–168; f) D. Ren, Y. Deng, A. D. Handoko, C. S. Chen, S. Malkhandi, B. S. Yeo, *ACS Catal.*, **2015**, *5*, 2814–2821; g) S. Ma, M. Sadakiyo, R. Luo, M. Heima, M. Yamauchi, P. J. A. Kenis, *J. Power Sources*, **2016**, *301*, 219–228; h) Y. Kwon, Y. Lum, E. L. Clark, J. W. Ager, A. T. Bell, *ChemElectroChem*, **2016**, *3*, 1012–1019.
- [6] F. Harnisch, C. Urban, *Angew. Chem.*, **2018**, *130*, 10168–10175.
- [7] a) A. Bar-Even, E. Noor, A. Flamholz, R. Milo, *Biochim. Biophys. Acta Bioenerg.*, **2013**, *1827*, 1039–1047; b) C. Gimkiewicz, R. Hegner, M. F. Gutensohn, C. Koch, F. Harnisch, *ChemSusChem*, **2017**, *10*, 958–967.
- [8] a) J. A. M. De Bont, R. A. J. M. Albers, *Antonie van Leeuwenhoek*, **1976**, *42*, 73–80; b) S. W. Ragsdale, E. Pierce, *Biochim. Biophys. Acta Proteins Proteom.*, **2008**, *1784*, 1873–1898; c) N. Kip, J. F. van Winden, Y. Pan, L. Bodrossy, G. Reichart, A. J. P. Smolders, M. S. M. Jetten, J. S. Sinninghe Damsté, H. J. M. Op den Camp, *Nat. Geosci.*, **2010**, *3*, 617–621; d) C. M. Spirito, H. Richter, K. Rabaey, A. J. M. Stams, L. T. Angenent, *Curr. Opin. Biotechnol.*, **2014**, *27*, 115–122.
- [9] J. G. Ferry, *FEMS Microbiol. Lett.*, **1990**, *87*, 377–382.
- [10] a) K. J. J. Steinbusch, H. V. M. Hamelers, C. M. Plugge, C. J. N. Buisman, *Energy Environ. Sci.*, **2011**, *4*, 216–224; b) M. Roghair, Y. Liu, D. P. B. T. B. Strik, R. A. Weusthuis, M. E. Bruins, C. J. N. Buisman, *Front. Bioeng. Biotechnol.*, **2018**, *6*, 50.
- [11] L. T. Angenent, H. Richter, W. Buckel, C. M. Spirito, K. J. J. Steinbusch, C. M. Plugge, D. P. B. T. B. Strik, T. I. M. Grootsholten, C. J. N. Buisman, H. V. M. Hamelers, *Environ. Sci. Technol.*, **2016**, *50*, 2796–2810.
- [12] a) P. He, W. Han, L. Shao, F. Lü, *Biotechnol. Biofuels*, **2018**, *11*, 4; b) V. De Groof, M. Coma, T. Arnot, D. J. Leak, A. B. Lanham, *Molecules*, **2019**, *24*, 398.
- [13] S. Sen, D. Liu, G. T. R. Palmore, *ACS Catal.*, **2014**, *4*, 3091–3095.
- [14] H. Li, P. H. Opgenorth, D. G. Wernick, S. Rogers, T. Wu, W. Higashide, P. Malati, Y. Huo, K. M. Cho, J. C. Liao, *Science*, **2012**, *335*, 1596.
- [15] Y. Tashiro, S. Hirano, M. M. Matson, S. Atsumi, A. Kondo, *Metab. Eng.*, **2018**, *47*, 211–218.
- [16] T. Haas, R. Krause, R. Weber, M. Demler, G. Schmid, *Nat. Can.*, **2018**, *1*, 32–39.
- [17] Y. X. Huang, Z. Hu, *Fuel*, **2018**, *220*, 8–13.
- [18] a) D. H. Won, H. Shin, J. Koh, J. Chung, H. S. Lee, H. Kim, S. I. Woo, *Angew. Chem.*, **2016**, 9297–9300; b) Z. Sun, T. Ma, H. Tao, Q. Fan, B. Han, *Chem*, **2017**, *3*, 560–587.
- [19] Y. Hori in *Modern Aspects of Electrochemistry*, Vol. 42 (Eds.: C. G. Vayenas, R. E. White, M. E. Gamboa-Aldeco), Springer, New York, **2008**, pp. 89–189.
- [20] Y. Jiang, N. Chu, W. Zhang, J. Ma, F. Zhang, P. Liang, R. J. Zeng, *Water Res.*, **2019**, *159*, 87–94.
- [21] C. W. Li, M. W. Kanan, *J. Am. Chem. Soc.*, **2012**, *134*, 7231–7234.
- [22] a) J. Wu, F. G. Risalvato, F. S. Ke, P. J. Pellechia, X. D. Zhou, *J. Electrochem. Soc.*, **2012**, *159*, F353–F359; b) X. Min, M. W. Kanan, *J. Am. Chem. Soc.*, **2015**, *137*, 4701–4708.
- [23] R. Kortlever, K. H. Tan, Y. Kwon, M. T. M. Koper, *J. Solid State Electrochem.*, **2013**, *17*, 1843–1849.
- [24] J. Zheng, W. Sheng, Z. Zhuang, B. Xu, Y. Yan, *Sci. Adv.*, **2016**, *2*, e1501602.
- [25] J. He, A. Huang, N. J. J. Johnson, K. E. Dettelbach, D. M. Weekes, Y. Cao, C. P. Berlinguette, *Inorg. Chem.*, **2018**, *57*, 14624–14631.
- [26] R. Kas, K. K. Hummadi, R. Kortlever, P. de Wit, A. Milbrat, M. W. J. Luiten-Olieman, N. E. Benes, M. T. M. Koper, G. Mul, *Nat. Commun.*, **2016**, *7*, 10748.
- [27] K. P. Kuhl, E. R. Cave, D. N. Abram, T. F. Jaramillo, *Energy Environ. Sci.*, **2012**, *5*, 7050–7059.
- [28] R. Kortlever, C. Balemans, Y. Kwon, M. T. M. Koper, *Catal. Today*, **2015**, *244*, 58–62.
- [29] Y. Hori, S. Suzuki, *J. Res. Inst. Catal. Hokkaido Univ.*, **1982**, *30*, 81–88.
- [30] Y. Hori, H. Konishi, T. Futamura, A. Murata, O. Koga, H. Sakurai, K. Oguma, *Electrochim. Acta*, **2005**, *50*, 5354–5369.
- [31] I. Bhugun, D. Lexa, J. M. Savéant, *J. Phys. Chem.*, **1996**, *100*, 19981–19985.
- [32] D. Hiltrop, S. Cychy, K. Elumeeva, W. Schuhmann, M. Muhler, *Beilstein J. Org. Chem.*, **2018**, *14*, 1428–1435.
- [33] E. Pérez-Gallent, G. Marcandalli, M. C. Figueiredo, F. Calle-Vallejo, M. T. M. Koper, *J. Am. Chem. Soc.*, **2017**, *139*, 16412–16419.
- [34] W. Tang, A. A. Peterson, A. S. Varela, Z. P. Jovanov, L. Bech, W. J. Durand, S. Dahl, J. K. Nørskov, I. Chorkendorff, *Phys. Chem. Chem. Phys.*, **2012**, *14*, 76–81.
- [35] X. Feng, K. Jiang, S. Fan, M. W. Kanan, *J. Am. Chem. Soc.*, **2015**, *137*, 4606–4609.
- [36] Z. Zaybak, J. M. Pisciotta, J. C. Tokash, B. E. Logan, *J. Biotechnol.*, **2013**, *168*, 478–485.
- [37] S. A. Patil, J. B. A. Arends, I. Vanwonterghem, J. van Meerbergen, K. Guo, G. W. Tyson, K. Rabaey, *Environ. Sci. Technol.*, **2015**, *49*, 8833–8843.
- [38] L. Jourdin, T. Grieger, J. Monetti, V. Flexer, S. Freguía, Y. Lu, J. Chen, M. Romano, G. G. Wallace, J. Keller, *Environ. Sci. Technol.*, **2015**, *49*, 13566–13574.
- [39] K. J. J. Steinbusch, H. V. M. Hamelers, C. J. N. Buisman, *Water Res.*, **2008**, *42*, 4059–4066.

Manuscript received: April 20, 2020  
Accepted manuscript online: April 29, 2020  
Version of record online: June 16, 2020